METHODS

The institutional ethics committee approved all experimental procedures. Animal care was conducted humanely in compliance with the Principles of Laboratory Animal Care (1).

ONO-1301NPs STABILITY IN ARTIFICIAL PLASMA

Artificial plasma [Dulbecco's phosphate-buffered saline (DPBS), calcium, magnesium; Manufacturer: Thermo; Buffer containing DPBS, Ca, Mg: solution not containing protein, enzymes or lipids] was cultured at 37℃ for 72 h, and ONO-1301 was separated from the ONO-1301NPs preparation by ultrafiltration [Stirring cell Model 8003, Manufacturer: Merck, Ultrafiltration membrane: cutoff molecular weight 300 kDa, room temperature (20~25℃), overnight (16 h) ultrafiltration process]. After deproteinization, each fraction was then measured with methanol using high performance liquid chromatography (HPLC). The results confirmed approximately 7% free ONO-1301. Lipoprotein lipase (Brand name: Lipoprotein lipase, Manufacturer: Fujifilm, Wako Pure Chemical Corporation) was cultured as the lipase enzyme, with an enzyme concentration of 10,000 units/mL (8.3 mg/mL) at 37℃ for 72 h, and then separated and measured using HPLC following a previously described method (2). The results confirmed approximately 55% free ONO-1301. However, separation of ONO-1301 due to ONO-1301NPs breakdown could not be confirmed with phospholipase A2 processing even after 72 h.

MEASUREMENT OF ONO-1301 CONCENTRATIONS IN PLASMA AND HEART. The rats from the ONO-solution and ONO-nanoparticle (NP) groups (n = 9 each) were humanely sacrificed to sample the plasma and the heart, which was divided into ischemic and non-ischemic parts, at 8 and 24 h after the reperfusion. The plasma was stored at −80 °C, and the

heart was thoroughly washed with phosphate-buffered saline and stored at −80 °C until HPLC–tandem mass spectrometry analysis (3) to measure ONO-1301 concentrations in the plasma and each part of the heart. The half-life of ONO-1301NPs was calculated using Phoenix WinNonlin version 7.0 (Certara L.P.).

INJECTION AND ANALYSIS OF FLUORESCENTLY LABELED NPS. The rats injected with fluorescently labeled NPs were humanely sacrificed 24 h after the injection. The harvested hearts were fixed with 4% paraformaldehyde and then embedded in OCT Compound and frozen under liquid nitrogen. Cryosections (5 μm) of a heart sample were analyzed by confocal microscopy (FLUOVIEW FV10i; Olympus, Tokyo, Japan).

***EX VIVO* MAGNETIC RESONANCE IMAGING.** The rats injected with Gadolisome or saline were anesthetized 24 h after the injection, and the anterior aspect of the rib cage was removed to obtain a clear view of the heart and great vessels. Then, an 18-gauge perfusion needle was passed through the ascending aorta to inject 4% paraformaldehyde into the heart after clamping the ascending aorta. The perfusion-fixed heart was excised and immersed in 4% paraformaldehyde. *Ex vivo* magnetic resonance imaging scanning of the excised rat heart was performed using an 11.7 Tesla vertical bore scanner (AVANCE II 500WB; Bruker BioSpin, Ettlingen, Germany) with a 15-mm inner diameter volume coil (4).

[^{13}N]-AMMONIA POSITRON EMISSION TOMOGRAPHY. The rats from the Sham (n = 4), Vehicle (n = 4), ONO-solution (n = 6), and ONO-NP (n = 6) groups were anesthetized with 2% isoflurane plus 100% oxygen at 2 L/min, and a Terumo 24-gauge indwelling cannula was inserted into the tail vein for [^{13}N]-ammonia myocardial perfusion for a positron emission tomography (PET)–computed tomography (CT) (Inveon MM; Siemens Medical Solutions,

Knoxville, Tennessee) study (5). The rats were placed in a feet-first prone position on the scanner warming bed. At rest, 37.1 ± 6.4 MBq of [^{13}N]-ammonia was injected via the tail vein, followed by a 0.75-mL saline flush. Dynamic imaging data acquisition started simultaneously with the injection and extended for 10 min. Fifteen minutes later, a selective adenosine A_{2A} receptor agonist (CGS-21680, 5 μg/kg; Abcam, Cambridge, Massachusetts) was injected to induce a hyperemic state (6). Five minutes after the adenosine injection, 72.0 ± 12.5 MBq of [^{13}N]-ammonia was injected, and stress dynamic imaging data were similarly acquired for 10 min. The CT data were acquired at a tube voltage of 80 kVp and current of 140 μA for scatter and attenuation correction before and after PET image acquisition. The systemic heart rate and blood pressure were measured indirectly using a noninvasive system (BP-98A-L; Softron, Japan) and a tail-cuff method.

The acquired PET–CT data was reconstructed using three-dimensional ordered-subset expectation maximization, followed by maximum a posteriori reconstruction (OSEM3D-MAP, 16 subsets, 2 OSEM3D, and 18 MAP iterations) with attenuation and scatter correction. The image matrix and voxel size were 128 × 128 × 159 and 0.776 × 0.776 × 0.796 mm, respectively. Volumes of interest were semi-automatically generated on the left and right ventricles using the PMOD software, version 3.604 (PMOD Technologies, Ltd., Zurich, Switzerland). The myocardium volumes of interest were segmented into 17 American Heart Association segments (7). The myocardial blood flow (MBF) of each segment was calculated using the one-tissue compartment model (8). Regional MBF was categorized as infarct, border, and remote region MBF according to the area of the ischemic insult (Online Figure 1B).

ENZYME-LINKED IMMUNOSORBENT ASSAY AND TRIPHENYLTETRAZOLIUM CHLORIDE–EVANS BLUE STAINING. Twenty-four h after myocardial ischemia/reperfusion, the rats were sacrificed to obtain blood samples for analyzing plasma

troponin I and the hearts for measuring the infarct size (Sham, n = 12; Vehicle, n = 11; ONO-solution, n = 13; ONO-NP, n = 12). The heart and femoral vein were exposed under general anesthesia and mechanical ventilation. First, 2 mL of blood was sampled from the femoral vein. The plasma was separated by centrifugation of the blood samples at 3,000 rpm for 10 min and stored at −80 °C. Cardiac troponin I was analyzed using a rat cardiac troponin I enzyme-linked immunosorbent assay kit (Life Diagnostics, Inc., West Chester, Pennsylvania) (9). Subsequently, 1.5 mL of 2% Evans Blue (Sigma–Aldrich, St. Louis, Missouri) was injected through the femoral vein immediately after re-occlusion of left anterior descending artery with the suture left *in situ*. The heart was then excised and cut parallel to the apex-base axis into three segments, which were incubated with 4% triphenyltetrazolium chloride (Sigma–Aldrich). The segment at the papillary muscle level was selected for evaluation. The area at risk of infarction (negative for Evans Blue), infarct area (negative for triphenyltetrazolium chloride), and the whole left ventricular area were assessed using a Leica M205FA fluorescence stereo microscope (Leica Microsystems, Wetzlar, Germany) in a blind manner. The infarct size (%) was calculated as (infarct area/area at risk of infarction) ×100 (10).

HISTOLOGY AND IMMUNOHISTOLABELING. The heart samples excised 24 h after reperfusion were fixed with 10% buffered formalin and embedded in paraffin (Sham, n = 10; Vehicle, n = 9; ONO-solution, n = 13; ONO-NP, n = 11). Slices (5 μm) of the paraffin-embedded sections were stained with periodic acid-Schiff to examine the degree of cardiomyocyte hypertrophy by optical microscopy (Leica). Myocyte sizes were determined by drawing point-to-point perpendicular lines across a cross-sectional area of the cell at the level of the nucleus. The heart sections were also stained with a rabbit polyclonal antibody to the von Willebrand factor (1:200, DAKO, Glostrup, Denmark) and a mouse monoclonal antibody to alpha-smooth muscle actin (1:50, DAKO) to assess the capillary density and capillary area, respectively. The

capillary density was calculated as the number of positively stained capillaries, while the capillary area was calculated as the total capillary area divided by the capillary number. Furthermore, the sections were stained with hematoxylin and eosin. The number of polymorphonuclear leukocytes per high-power field was calculated as an indication of the degree of acute myocardial inflammation (10). These quantitative morphometric values were obtained from 10 randomly selected fields of the area at risk of infarction in each section and analyzed using the Metamorph software (Molecular Devices, Sunnyvale, California) (11).

REAL-TIME POLYMERASE CHAIN REACTION. The border areas of the excised heart samples (Sham, n = 10; Vehicle, n = 9; ONO-solution, n = 13; ONO-NP, n = 11) were immersed in RNA later (Thermo Fisher Scientific, Waltham, Massachusetts). Total RNA was isolated from the border area using the RNeasy kit (Qiagen, Hilden, Germany) and then reverse-transcribed using the Omniscript reverse transcriptase (Qiagen). Real-time polymerase chain reaction was performed using the TaqMan gene expression assay master mix (Thermo Fisher Scientific) on a 7500 Fast real-time polymerase chain reaction system (Thermo Fisher Scientific). The following genes were analyzed using TaqMan gene expression assays (Thermo Fisher Scientific): *Vegf* (Rn01511601_m1), hepatocyte growth factor (Rn00566673_m1), platelet-derived growth factor-β (Rn01502596_m1), angiopoietin-1 (*Ang-1*, Rn00585552_m1), stromal cell-derived factor-1 (Rn00573260_m1), interleukin-1β (Rn00580432_m1), interleukin-6 (Rn01410330_m1), and tumor necrosis factor-α (Rn01525859_g1). Glyceraldehyde-3-phosphate dehydrogenase (Rn01775763_g1) was coamplified as an internal control. Relative gene expression was determined using the ΔΔCt method.

REFERENCES

1. Carbone L. Pain management standards in the eighth edition of the Guide for the Care and Use of Laboratory Animals. J Am Assoc Lab Anim Sci 2012;51:322–8.

2. Morita SY, Ueda K, Kitagawa S. Enzymatic measurement of phosphatidic acid in cultured cells. J Lipid Res 2009;50:1945–52.

3. Saini GS, Wani TA, Gautam A, et al. Validation of the LC-MS/MS method for the quantification of mevalonic acid in human plasma and determination of the matrix effect. J Lipid Res 2006;47:2340–5.

4. Mori Y, Chen T, Fujisawa T, et al. From cartoon to real time MRI: in vivo monitoring of phagocyte migration in mouse brain. Sci Rep 2014;4:6997.

5. Bao Q, Newport D, Chen M, Stout DB, Chatziioannou AF. Performance evaluation of the inveon dedicated PET preclinical tomograph based on the NEMA NU-4 standards. J Nucl Med 2009;50:401–8.

6. Kawamura M, Paulsen MJ, Goldstone AB, et al. Tissue-engineered smooth muscle cell and endothelial progenitor cell bi-level cell sheets prevent progression of cardiac dysfunction, microvascular dysfunction, and interstitial fibrosis in a rodent model of type 1 diabetes-induced cardiomyopathy. Cardiovasc Diabetol 2017;16:142.

7. Cerqueira MD, Weissman NJ, Dilsizian V, et al. Standardized myocardial segmentation and nomenclature for tomographic imaging of the heart. a statement for healthcare professionals from the Cardiac Imaging Committee of the Council on Clinical Cardiology of the American

Heart Association. Circulation 2002;105:539–42.

8. DeGrado TR, Hanson MW, Turkington TG, et al. Estimation of myocardial blood flow for longitudinal studies with ^{13}N-labeled ammonia and positron emission tomography. J Nucl Cardiol 1996;3:494–507.

9. Cheng K, Malliaras K, Li TS, et al. Magnetic enhancement of cell retention, engraftment, and functional benefit after intracoronary delivery of cardiac-derived stem cells in a rat model of ischemia/reperfusion. Cell Transplant 2012;21:1121–35.

10. Fukushima S, Coppen SR, Varela-Carver A, et al. A novel strategy for myocardial protection by combined antibody therapy inhibiting both P-selectin and intercellular adhesion molecule-1 via retrograde intracoronary route. Circulation 2006;114:I251–6.

11. Shudo Y, Miyagawa S, Ohkura H, et al. Addition of mesenchymal stem cells enhances the therapeutic effects of skeletal myoblast cell-sheet transplantation in a rat ischemic cardiomyopathy model. Tissue Eng Part A 2014;20:728–39.

ONLINE FIGURE LEGENDS

ONLINE FIGURE 1 Study Design

(A) Study protocol. **(B)** Definition of the infarct, border, and remote areas.

LAD = left anterior descending artery; PBS = phosphate-buffered saline; NP = nanoparticle

ONLINE FIGURE 2 Characteristics of NPs containing (A) Empty, (B) Fluorescently labeled, and (C) Gadolisome

Average particle diameter was obtained by the dynamic light scattering method.

NP = nanoparticle; PDI = polydispersity index

ONLINE FIGURE 3 Retention rate of ONO-1301 (μg)/lipids (mg) between 0 with 72 h after processing with (A) D-PBS, (B) Lipoprotein lipase, and (C) Phospholipase A2

ONO-1301NPs undergoes hydrolysis by the lipase in plasma (mainly lipoprotein lipase) and the free ONO-1301 gradually separates. The separation rate of ONO-1301 through hydrolysis from ONO-1301NPs was 55% after 72 h, with 0 h data being 100%.

D-PBS = Dulbecco's phosphate-buffered saline

ONLINE FIGURE 4 Changes in Plasma Levels of Radioactivity Upon Intravenous Administration of [^{14}C]-ONO-1301 to Normal Male Rats (n = 4)

Upon administration of 0.1, 0.3, 1.0, and 3.0 mg/kg [^{14}C]-ONO-1301, the plasma levels of radioactivity increased in a dose-dependent-manner and showed linearity, without variation of the pharmacological half-time in each group. However, at a dose of 10 mg/kg, the plasma concentration revealed a prolonged half-life at an early period, and the area under the curve also increased more than expected, with a non-linear plasma concentration.

ONLINE TABLE 1 Kinetic Parameters of Intravenous Administration of ^{14}C-ONO-1301 to Normal Male Rats (n = 4)

Dose (mg/kg)	$AUC_{(0-\infty)}$ (ng eq · h/mL)	$T_{1/2\ (2-15\ min)}$ (min)	$T_{1/2\ (2-6\ h)}$ (h)	CL_{total} (mL/h·kg)
0.1	155.1 ± 19.8	5.38 ± 0.47	2.31 ± 0.88	653.7 ± 94.6
0.3	578.4 ± 104.3	5.67 ± 0.50	2.32 ± 0.27	532.0 ± 90.9
1.0	1,686.9 ± 124.6	6.76 ± 0.81	1.84 ± 0.20	595.4 ± 47.3
3.0	4,781.4 ± 130.4	7.31 ± 0.99	2.06 ± 0.39	627.8 ± 17.6
10	45,124.6 ± 5,555.1	14.45 ± 2.01	1.96 ± 0.17	224.4 ± 30.1

Values are mean ± standard deviation.

AUC = area under the curve; *CL* = clearance; $T_{1/2}$ = elimination half-life.

(A) Vehicle

Average particle diameter (nm)	PDI	Zeta potential (mV)	Lipids (mg/ml)
97.9	0.051	-17.9	42.0

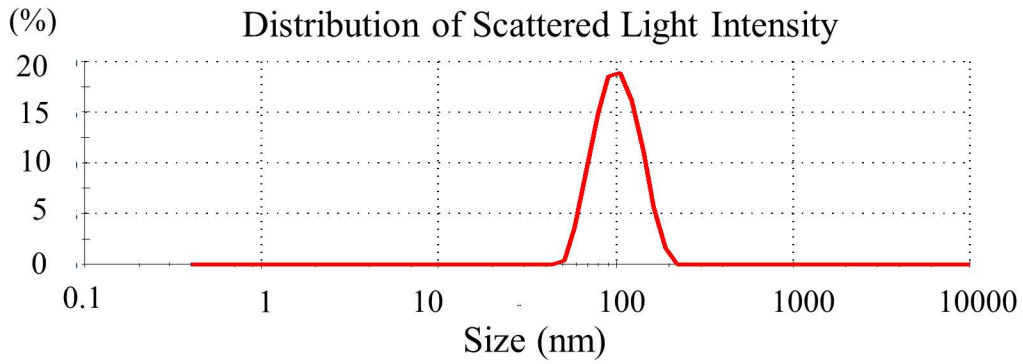

(B) fluorescently labeled NP

Average particle diameter (nm)	PDI	Zeta potential (mV)	Lipids (mg/ml)
134	0.194	-24	47.0

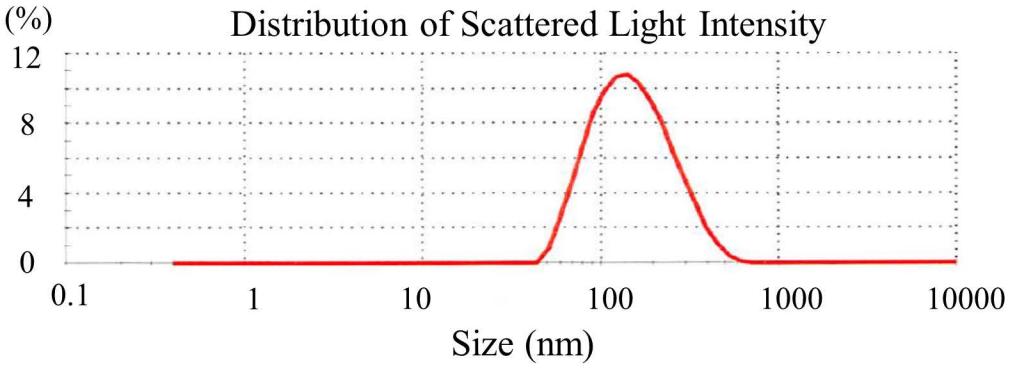

(C) Gadolisome

Average particle diameter (nm)	PDI	Zeta potential (mV)	Lipids (mg/ml)
127.4	0.126	-50.5	22.7

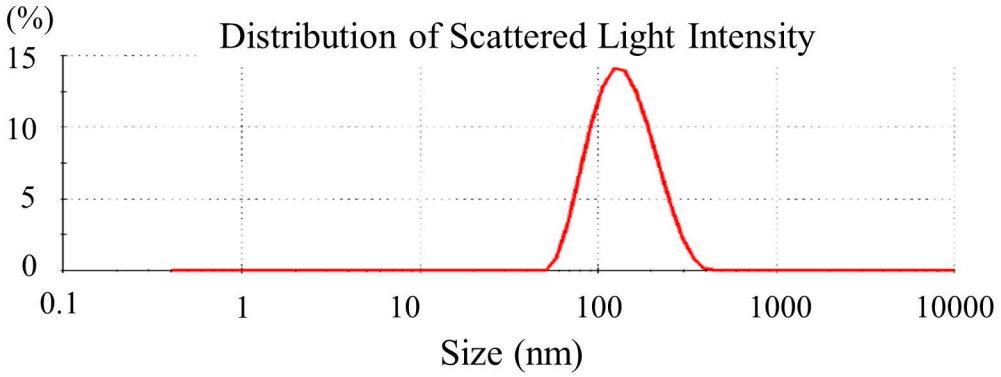

(A)

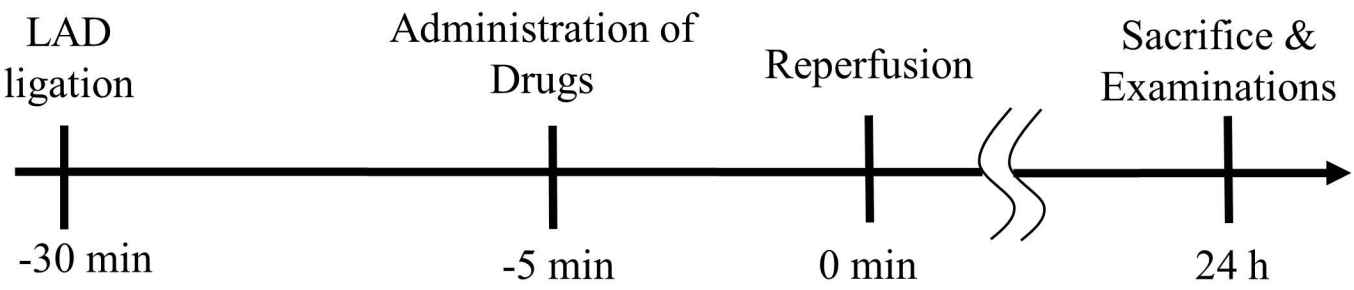

- PBS (5 mL/kg); Sham group
- NP alone (3 mg/kg); Vehicle group
- ONO-1301 solution (3 mg/kg); ONO-Solution group
- ONO-1301 NP (3 mg/kg); ONO-NP group

(B)

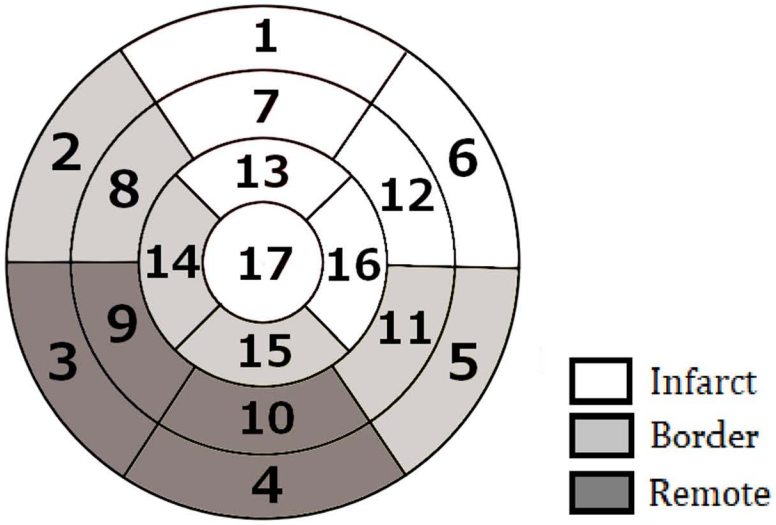

(A) D-PBS processing

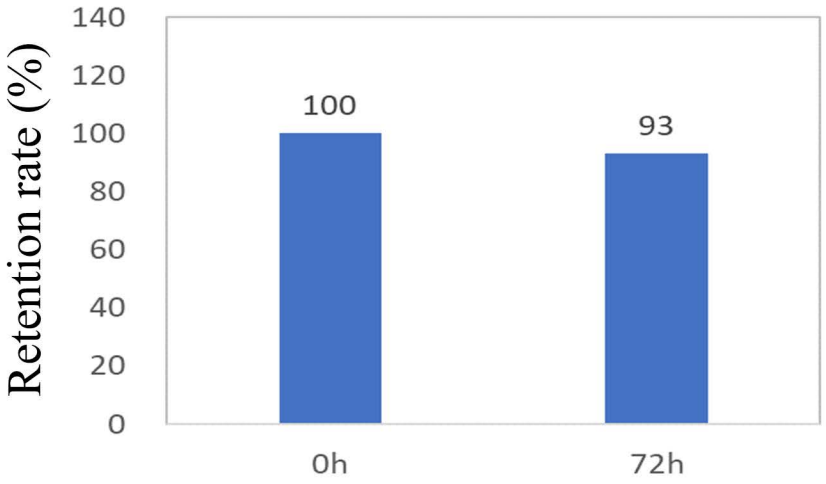

(B) Lipoprotein lipase processing

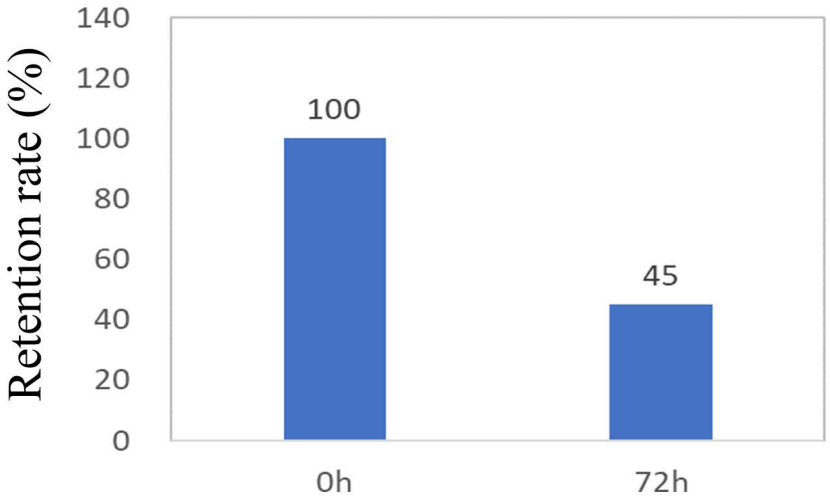

(C) Phospholipase A2 processing

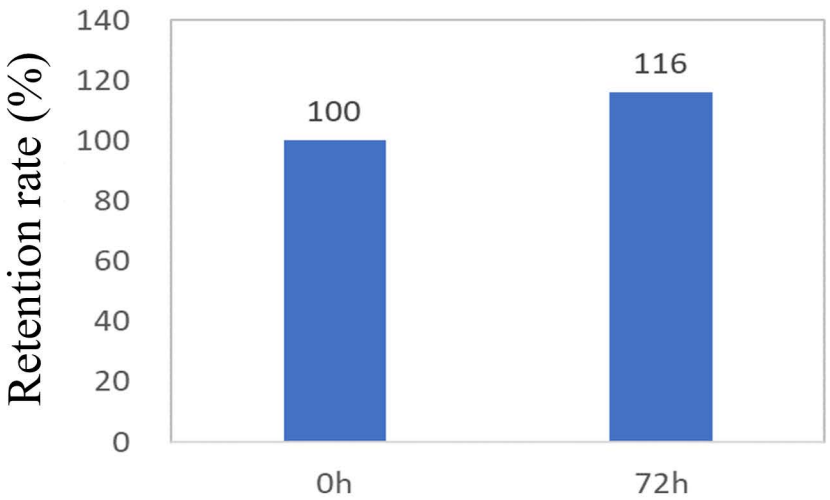

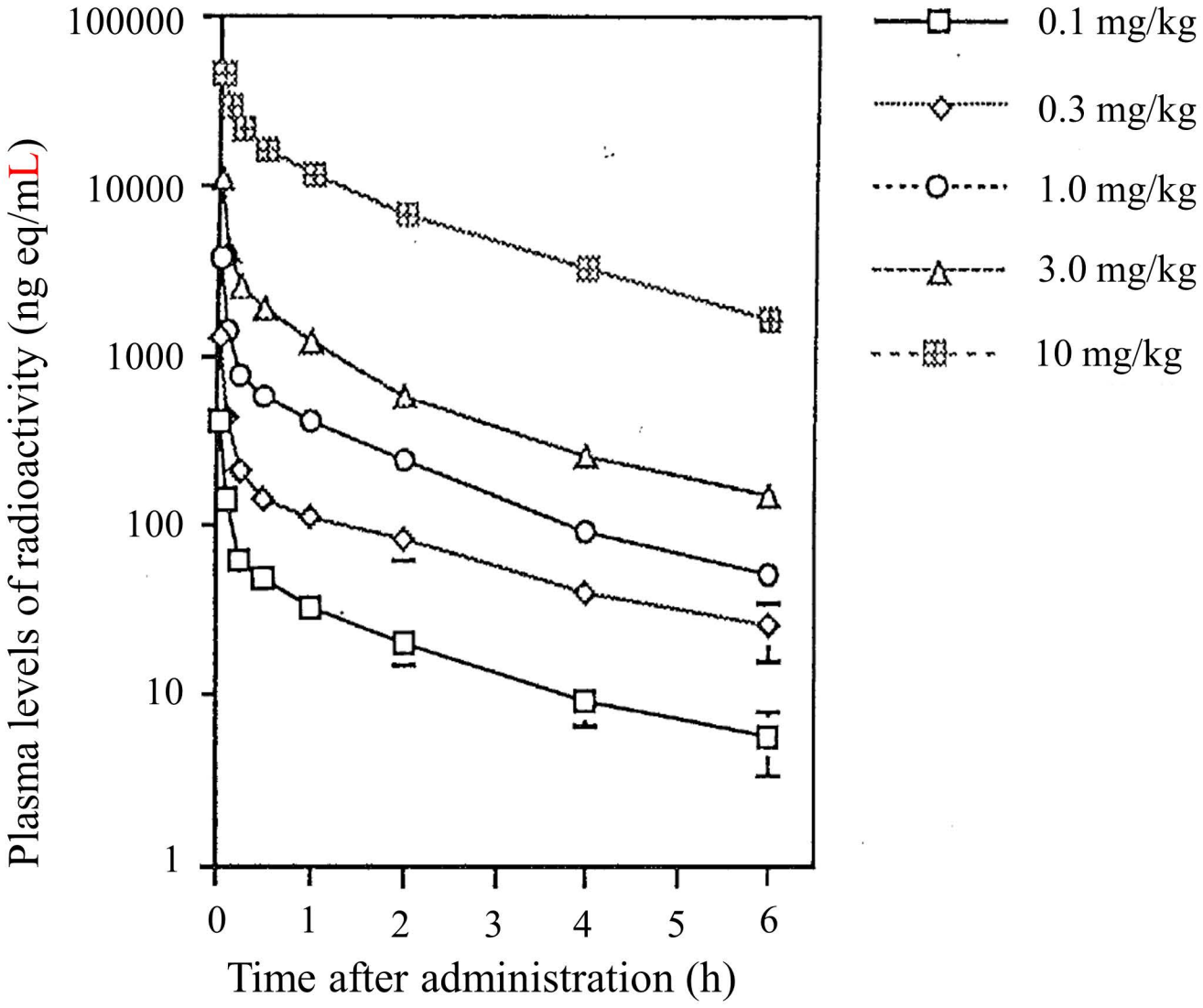
100000
10000
1000
100
10
1
Plasma levels of radioactivity (ng eq/mL)
0
1
2
3
4
5
6
Time after administration (h)
0.1 mg/kg
0.3 mg/kg
1.0 mg/kg
3.0 mg/kg
10 mg/kg